Experiments in Fluids (2006) 40: 188–195
DOI 10.1007/s00348-005-0049-x

RESEARCH ARTICLE

J. S. Connelly · M. P. Schultz · K. A. Flack

Velocity-defect scaling for turbulent boundary layers with a range of relative roughness

Received: 20 June 2005 / Revised: 17 August 2005 / Accepted: 2 September 2005 / Published online: 6 December 2005
© Springer-Verlag 2005

Abstract Velocity profile measurements in zero pressure gradient, turbulent boundary layer flow were made on a smooth wall and on two types of rough walls with a wide range of roughness heights. The ratio of the boundary layer thickness (δ) to the roughness height (k) was $16 \le \delta/k \le 110$ in the present study, while the ratio of δ to the equivalent sand roughness height (k_s) ranged from $6 \le \delta/k_s \le 91$. The results show that the mean velocity profiles for all the test surfaces agree within experimental uncertainty in velocity-defect form in the overlap and outer layer when normalized by the friction velocity obtained using two different methods. The velocity-defect profiles also agree when normalized with the velocity scale proposed by Zagarola and Smits (J Fluid Mech 373:33–70, 1998). The results provide evidence that roughness effects on the mean flow are confined to the inner layer, and outer layer similarity of the mean velocity profile applies even for relatively large roughness.

List of symbols

B	Smooth wall log-law intercept = 5.0
B_1	Velocity-defect intercept = $2\Pi/\kappa$
k	Roughness height
k_s	Equivalent sand roughness height
K	Acceleration parameter = $\frac{\nu}{U_e^2}\frac{dU_e}{dx}$
Re_x	Reynolds number based on the distance from leading edge = $U_e x/\nu$
Re_θ	Momentum thickness Reynolds number = $U_e\theta/\nu$
U	Mean velocity in the x direction
U_e	Freestream velocity
U_τ	Friction velocity = $\sqrt{\tau_w/\rho}$
ΔU^+	Roughness function
$-\overline{u'v'}$	Reynolds shear stress
x	Streamwise distance from plate leading edge
y	Normal distance from the effective origin
δ	Boundary layer thickness (y at $U = 0.995U_e$)
δ^*	Displacement thickness = $\int_0^\delta \left(1 - \frac{U}{U_e}\right) dy$
κ	von Kármán constant = 0.41
ν	Kinematic viscosity of the fluid
Π	Wake parameter
θ	Momentum thickness = $\int_0^\delta \frac{U}{U_e}\left(1 - \frac{U}{U_e}\right) dy$
ρ	Density of the fluid
τ_w	Wall shear stress
ω	Wake function

Superscript

$+$	Inner variable (normalized with U_τ or ν/U_τ)

J. S. Connelly · M. P. Schultz (✉)
Naval Architecture & Ocean Engineering Department, United States Naval Academy , Annapolis, MD 21402, USA
E-mail: mschultz@usna.edu

K. A. Flack
Mechanical Engineering Department,
United States Naval Academy, Annapolis, MD 21402, USA

1 Introduction

Surface roughness plays an important role in a variety of engineering applications. It can have a significant effect on the frictional losses in pipes, the drag on ships and aircraft, and the heat transfer in heat exchangers. For this reason, wall-bounded shear flows with roughness have been the focus of a large body of research. Reviews of much of this work are given by Raupach et al. (1991) and Jiménez (2004). The conclusion of both reviews based on a majority of both the experimental and computational evidence is that the flow structure is unaffected by surface roughness in the outer region of the shear layer. This supports the wall similarity hypothesis of Townsend (1976), which states that the

turbulence structure is unaffected by the surface condition at a sufficient distance from the wall. This distance is generally thought to be 3–5 roughness heights (k) from the wall (Raupach et al. 1991; Flack et al. 2005). The underlying assumptions of Townsend's hypothesis are that the Reynolds number is sufficiently high and that k is small compared to the shear layer thickness. The question of outer layer similarity is of practical interest since most computational models for rough walls rely at some level on the similarity between smooth and rough wall flows (Patel 1998).

Recently, compelling support for outer layer similarity in internal flows has been offered. Bakken et al. (2005) showed that very little roughness effect can be observed outside of $5k$ in the mean flow and turbulence statistics up to third-order moments in fully developed channel flow. Shockling et al. (2005) found that the mean velocity profiles for smooth and rough pipes are similar in the outer layer for a very large range of Reynolds number. The unique contribution of this study was that it documented the mean flow in a single rough pipe from the hydraulically smooth flow regime to the fully rough flow regime in which k was a very small fraction of the pipe diameter, therefore, more closely following the underlying assumptions of Townsend's hypothesis than previous investigations.

Outer layer similarity in turbulent boundary layers has been the topic of more contentious debate. A recent study by Flack et al. (2005) shows support for outer layer similarity in both the mean flow and turbulence statistics for smooth and rough walls. However, several studies (e.g. Krogstad et al. 1992; Keirsbulck et al. 2002; Akinlade et al. 2004) have shown differences in the mean flow over rough walls extending well into the outer layer. Some researches (e.g. Krogstad and Antonia 1999; Keirsbulck et al. 2002) have also observed that roughness affects the turbulence structure far from the wall. Jiménez (2004) attempted to reconcile these differences by contending that outer layer similarity can only be expected if k is sufficiently small compared to the boundary layer thickness, δ, as is assumed in Townsend's hypothesis. He states that for similarity in the outer region to exist, $\delta/k \geq 40$. The recent experimental investigation of Flack et al. (2005) largely supports the conclusions of Jiménez. However, they state that since the equivalent sand roughness height, k_s, better represents the effect of the roughness on the mean flow than k, it should be used instead of the roughness height to evaluate the existence of outer similarity. Based on a review of existing data, they offer that $\delta/k_s \geq 40$ be the criteria for outer layer similarity to hold. Another possible explanation of the confounding results observed for rough wall boundary layers is offered by Bakken et al. (2005). They state that roughness effects observed in the outer region of turbulent boundary layers, which are absent in rough wall internal flows, may simply be a result of the difference in the outer boundary condition in the two flows. In boundary layer flows over roughness, there is an increase in the growth rate and entrainment of irrotational flow, which can affect diffusion in the outer layer. This is absent in symmetrically roughened channels and pipes.

In light of the disparate findings for rough wall turbulent boundary layers, the purpose of the present experimental investigation is to critically evaluate the applicability of outer layer similarity in the mean velocity profiles for these flows with a large range of relative roughness (δ/k or δ/k_s). In this study, the mean velocity profiles for rough surfaces with $16 \leq \delta/k \leq 110$ ($6 \leq \delta/k_s \leq 91$) are compared to that for a smooth wall. From these results, it is hoped that the range of relative roughness in which outer layer similarity in the mean flow can be expected to hold will be identified.

2 Mean flow scaling

The flow in a smooth wall turbulent boundary layer can be broken into two regions: the inner and outer layers, each having its own scaling law. In the inner layer, the mean velocity, U, at a given distance from the wall, y, is determined by the friction velocity, U_τ, and the kinematic viscosity, ν, such that (Schubauer and Tchen (1961)

$$U = f_1(y, U_\tau, \nu). \tag{1}$$

In non-dimensional form this becomes the "law of the wall", given as

$$U^+ = f(y^+), \tag{2}$$

where $U^+ = U/U_\tau$, $y^+ = yU_\tau/\nu$, $U_\tau = (\tau_w/\rho)^{1/2}$, τ_w = wall shear stress, and ρ = fluid density. In the outer region, the difference between the velocity at the outer edge of the boundary layer, U_e, and the local mean velocity, U, at a distance y from the wall is determined by the boundary layer thickness, δ, and U_τ, such that (von Kármán (1930)

$$U_e - U = g_1(y, \delta, U_\tau). \tag{3}$$

In non-dimensional form this becomes the "velocity-defect law", given as

$$U_e^+ - U^+ = g(\eta), \tag{4}$$

where $U_e^+ = U_e/U_\tau$ and $\eta = y/\delta$.

Millikan (1938) proposed, by matching the velocity profiles in the law of the wall (Eq. 2) and the velocity-defect law (Eq. 4), that a logarithmic velocity distribution results in the overlap region ($\delta >> y >> \nu/U_\tau$) at sufficiently high Reynolds number. This is termed the "log-law" and for a smooth wall turbulent boundary layer, is given by

$$U^+ = \frac{1}{\kappa}\ln(y^+) + B, \tag{5}$$

where κ = von Kármán constant ≈ 0.41 and B = smooth wall log-law intercept ≈ 5.0. In terms of the

velocity defect, the logarithmic region can be expressed as

$$U_e^+ - U^+ = -\frac{1}{\kappa}\ln(\eta) + B_1, \tag{6}$$

where B_1 = velocity-defect intercept = $2\Pi/\kappa$ and Π = wake strength.

Clauser (1954) and Hama (1954) found that the effect of surface roughness on the mean flow was confined to the inner layer, causing a downward shift in the log-law (Eq. 5) called the roughness function, ΔU^+. Equation 5 can, therefore, be recast for rough wall boundary layers as:

$$U^+ = \frac{1}{\kappa}\ln(y^+) + B - \Delta U^+. \tag{7}$$

Coles (1956) extended the log-law to cover both the overlap and outer region of the boundary layer by introducing a wake function, ω. This is termed the "law of the wake". For smooth and rough wall boundary layers, it is given as Eqs. 8 and 9, respectively:

$$U^+ = \frac{1}{\kappa}\ln(y^+) + B + \frac{\Pi}{\kappa}\omega(\eta), \tag{8}$$

$$U^+ = \frac{1}{\kappa}\ln(y^+) + B - \Delta U^+ + \frac{\Pi}{\kappa}\omega(\eta). \tag{9}$$

Both Clauser (1954) and Hama (1954) observed that mean velocity in the outer region expressed in velocity-defect form (Eqs. 4, 6) was independent of surface roughness. Using the wake function, velocity-defect scaling can be extended to describe the overlap and outer region of the boundary layer for both smooth and rough wall boundary layers as:

$$U_e^+ - U^+ = -\frac{1}{\kappa}\ln(\eta) + B_1 - \frac{\Pi}{\kappa}\omega(\eta). \tag{10}$$

The similarity in the mean velocity in the outer layer can, therefore, be assessed using velocity-defect scaling. Collapse of mean velocity profiles in this form will indicate that roughness effects on the mean flow are confined to the inner layer. Lack of collapse will show that roughness effects propagate into the outer region of the boundary layer.

3 Experimental facilities and method

The present experiments were made in the closed circuit water tunnel facility at the United States Naval Academy Hydromechanics Laboratory. The test section is 40 cm by 40 cm in cross-section and 1.8 m in length, with a tunnel velocity range of 0–8.0 m/s. The current tests were run at a tunnel speed of ~2.0 m/s ($Re_x = 2.7\times10^6$). The freestream turbulence intensity in the tunnel is ~0.5%. Further details of the water tunnel facility are given in Schultz and Flack (2003) and Flack et al. (2005). Seven surfaces were tested in this study, as listed in Table 1. One was a smooth cast acrylic surface. The other six were rough surfaces. Three surfaces were covered with wet/dry sandpaper. These included 80, 24 and 12-grit sandpaper. The remaining three were covered with woven wire mesh with pitch-to-diameter ratios of 6.25 for M1, 4.58 for M2, and 8.45 for M3. The roughness height, k, given in Table 1 is the maximum peak to trough height measured over a 50 mm^2 sampling area. For the sandpaper surfaces, this was measured using a dial indicator. For the mesh surfaces, it was taken to be twice the wire diameter. The test fixture is the same as that used by Schultz and Flack (2003, 2005). The forward most 200 mm of the plate is covered with 36-grit sandpaper to trip the developing boundary layer. The test specimen mounts flush into the test fixture and its forward edge is located immediately downstream of the trip. The boundary layer profiles presented here were taken 1.35 m downstream of the leading edge of the test fixture. Profiles taken from 0.90 m to the measurement location confirmed that the mean flow had reached self-similarity as witnessed by the collapse of the streamwise velocity-defect profiles. The upper wall of the test section was adjusted to counteract the physical growth of the boundary layer in order to maintain a nearly zero pressure gradient ($K \le 2\times10^{-8}$). A schematic of the water tunnel test fixture is shown in Fig. 1.

Velocity measurements were made using a TSI FSA3500 two-component, fiber-optic laser Doppler velocimeter (LDV). The LDV used a four-beam arrangement and was operated in backscatter mode. The measurement volume diameter was 90 m and its length was 1.3 mm. The viscous length scale (ν/U_τ) varied from

Table 1 Experimental test conditions

Surface	Designation	K (mm)	U_e (m/s)	Re_θ	U_τ, Clauser chart (m/s)	U_τ, total stress (m/s)	δ (mm)	δ* (mm)	θ (mm)	Π	k^+	k_s^+	ΔU^+	δ/k	δ/k_s
Smooth wall	Smooth wall	–	2.00	6,570	0.0757	0.0746	30.8	4.37	3.28	0.48	–	–	–	–	–
Mesh #1	M1	0.320	1.99	7,280	0.0981	0.0951	34.8	5.73	4.05	0.41	28	56	6.3	110	55
80-Grit sandpaper	S1	0.690	1.98	7,960	0.0917	0.0901	37.2	5.86	4.21	0.43	60	36	5.3	54	91
Mesh #2	M2	1.40	2.00	9,100	0.119	0.113	38.3	7.71	4.99	0.46	150	370	10.9	27	11
24-Grit sandpaper	S2	1.80	1.99	8,950	0.120	0.119	37.9	7.68	4.94	0.42	200	360	10.8	21	11
Mesh #3	M3	2.45	2.00	13,040	0.133	0.126	46.8	10.5	6.39	0.48	330	1,150	13.7	19	5.5
12-Grit sandpaper	S3	2.85	2.00	12,490	0.132	0.131	44.9	9.86	6.11	0.38	380	860	13.0	16	7.0

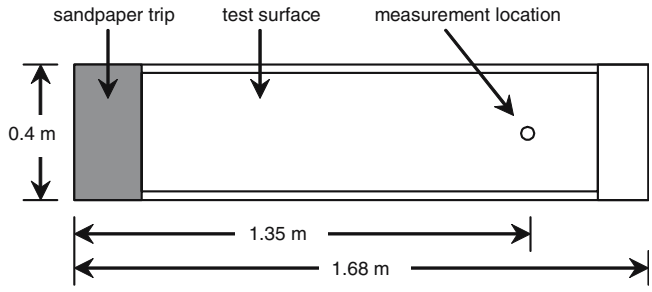

Fig. 1 Schematic of the flat plate test fixture

7.5 μm for the roughest wall to 13 μm for the smooth wall. The diameter of the probe volume, therefore, ranged from 7 to 13 viscous length scales in the present study. The LDV probe was mounted on a Velmex three-axis traverse unit. The traverse allowed the position of the probe to be maintained to ±5 μm in all directions. In order to facilitate two components, near wall measurements, one of the vertical beams was redirected by a beam displacer on the LDV probe, aligning the beam parallel to the test surface. This eliminated the need for tilting or rotating the probe as was done in previous studies in the facility (Schultz and Flack 2003, 2005; Flack et al. (2005). Velocity measurements were conducted in coincidence mode with 50,000 random samples per location. Doppler bursts for the two channels were required to fall within a 100 μs coincidence window or the sample was rejected.

In this study, the friction velocity, U_τ, for the smooth surface was found using the Clauser chart method with log-law constants $\kappa = 0.41$ and $B = 5.0$. This was confirmed using the measurement of velocity gradient in the linear sublayer. The agreement between the two methods was within 1%. For the rough walls, U_τ was obtained using a procedure based on the modified Clauser chart method given by Perry and Li (1990). Data from $y^+ \geq 100$ and $y/\delta \leq 0.125$ were used. First, the location of the virtual origin was determined by assuming that a linear log-layer exists in U/U_e versus $\ln(yU_e/\nu)$. Next, U_τ was found using the slope of this log-layer. This is given as

$$U_\tau = \kappa U_e \left[\frac{\partial\left(\frac{U}{U_e}\right)}{\partial\left(\ln\left(\frac{yU_e}{\nu}\right)\right)} \right]. \tag{11}$$

The strength of the wake, Π, was then determined using the departure of the mean velocity profile from a logarithmic distribution in the outer layer. Further details of the procedure are given in Schultz and Flack (2003). The total stress method was also used to determine U_τ for all the test surfaces. It assumes a constant stress region equal to the wall shear stress that exists in the overlap and inner region of the boundary layer. Using a sum of the viscous and turbulent shear stresses evaluated at the total stress plateau in the overlap and inner layer, U_τ may be determined as

$$U_\tau = \left[\nu \frac{\partial U}{\partial y} - \overline{u'v'} \right]^{1/2}. \tag{12}$$

The results from the modified Clauser chart and the total stress methods agreed to within 5% for all surfaces tested, well within the combined experimental uncertainty.

4 Uncertainty estimates

Precision uncertainty estimates for the velocity measurements were made through repeatability tests using the procedure given by Moffat (1988). The 95% confidence bounds for flow quantities were obtained using the standard procedure outlined in Coleman and Steele (1995). LDV measurements are susceptible to a variety of bias errors as detailed by Edwards (1987). The LDV bias corrections applied to the present data were similar to those used in previous studies by the authors and are detailed in Flack et al. (2005). The resulting overall uncertainty in the mean velocity is ±1%. The uncertainty in U_τ using the Clauser chart method is ±3% for the smooth wall and ±5% for the rough walls. The uncertainty in U_τ using the total stress method is ±7% for both the smooth and rough walls. The uncertainty bounds for δ, δ*, and θ are ±6, ±4, and ±5%, respectively. The uncertainty in Π is ±10% for the smooth wall and ±15% for the rough walls.

5 Results and discussion

5.1 Experimental conditions and bulk flow parameters

The test conditions for the present study are shown in Table 1. Re_θ varied from 6,570 for the smooth wall to 13,040 for the M3 surface. These all exceed the criteria for the existence of a fully developed turbulent boundary layer of $Re_\theta > 6{,}000$ given by Coles (1962). Accurate determination of U_τ is important since it is typically used as the normalizing velocity scale in velocity-defect scaling. Inaccuracies in U_τ could, therefore, lead to erroneous conclusions about outer layer similarity in the mean flow over rough and smooth walls. It should be stated that determination of U_τ from the log-law is more problematic and has greater experimental uncertainty for rough walls than smooth walls. This is largely due to the fact that the location of the effective origin and the roughness function are additional parameters that must be determined for rough walls (Acharya et al. 1986). It is important, therefore, to verify the friction velocity determined by the Clauser chart with another independent method. In this case, the total stress method, which makes no assumptions about the existence of a linear log-law profile, was used. The values of U_τ obtained using the Clauser chart and the total stress methods agreed to within 5% for all the test surfaces.

The physical growth of the boundary layer was significantly higher on the rough walls. The displacement

thickness (δ^*) was the most affected of the boundary layer length scales, showing increases of 31–126% for the rough walls. The momentum thickness (θ) displayed increases of 23–86% above the smooth wall value, while the boundary layer thickness (δ) increased 13–46% on the rough walls. The wake strength (Π) for the smooth wall was 0.48. This is slightly less than 0.55, the value given by Coles (1956) as the high Reynolds number asymptote for smooth walls. This may have resulted from the slightly elevated freestream turbulence level (~0.5%) in the present test facility, although the more recent smooth wall data of DeGraaff and Eaton (2000) indicates that Π may decrease very slightly with Reynolds number for $Re_\theta > 5{,}200$. All the values of Π for the rough walls are at or slightly below the smooth wall value. However, the differences in Π observed with surface condition are within the combined uncertainty of the measurements and do not show any trend with increasing roughness height. The results of Krogstad et al. (1992), Keirsbulck et al. (2002), and Akinlade et al. (2004) showed that Π was increased for rough wall flows. Krogstad et al. (1992) attributed the increase to greater entrainment of irrotational fluid for rough wall flows. No significant change in Π was observed in the rough wall studies of Bandyopadhyay (1987) and Ligrani and Moffat (1986).

The roughness Reynolds number based on the equivalent sand roughness height, k_s^+, is shown in Table 1. The equivalent sand roughness height, k_s, is discussed in Schlichting (1979) and represents the roughness height in Nikuradse's (1933) experiments on monodisperse sandgrains in the fully rough flow regime that gives the same roughness function as the roughness of interest. This was calculated using the formulation of Ligrani and Moffat (1986), given as

$$\Delta U^+ = \frac{1}{\kappa}\ln\left(k_s^+\right) + B - C, \tag{13}$$

where C = rough wall log-law intercept in relative roughness form = 8.5 (Ligrani and Moffat 1986). Based on the criteria of Schlichting (1979), the present rough walls span the range from the transitionally rough ($5 \le k_s^+ \le 70$) to the fully rough flow regime ($k_s^+ > 70$). The relative roughness used in this study was $16 \le \delta/k \le 110$ and $6 \le \delta/k_s \le 91$ based on the roughness height and the equivalent sand roughness height, respectively. Therefore, the smallest roughness is more than an order of magnitude smaller than the inner layer thickness, while the largest roughness is a substantial fraction of the inner layer thickness.

5.2 Mean velocity profiles

The mean velocity profiles for all the test surfaces are presented in outer variables in Fig. 2. The smooth wall results of DeGraaff and Eaton (2000) taken at $Re_\theta = 5{,}200$ are presented for comparison. The present smooth wall results agree within experimental uncertainty with those of DeGraaff and Eaton. The rough walls all display profiles that are not as full as the smooth wall profiles, indicative of the increased momentum deficit on the rough walls. This deficit is observed to increase with roughness height. The mean velocity profiles for all the test surfaces in inner coordinates are shown in Fig. 3. The values of U_τ used to normalize the data were determined using the Clauser chart method. Again, the smooth wall data of DeGraaff and Eaton (2000) taken at $Re_\theta = 5{,}200$ are also shown. The present smooth wall profile displays good agreement with a linear sublayer ($y^+ = U^+$) for $y^+ \le 5$. The smooth wall profile also shows excellent agreement with the results of DeGraaff and Eaton from linear sublayer to the outer edge of the overlap region. In the wake region, the agreement is not quite as good, although still within experimental uncertainty. This may simply be due to either the higher Re_θ in the present study or the slightly elevated freestream turbulence intensity in the test facility. The velocity profiles for the rough walls exhibit a downward shift or roughness function, ΔU^+, which increases with roughness height. The present data support the concept that both

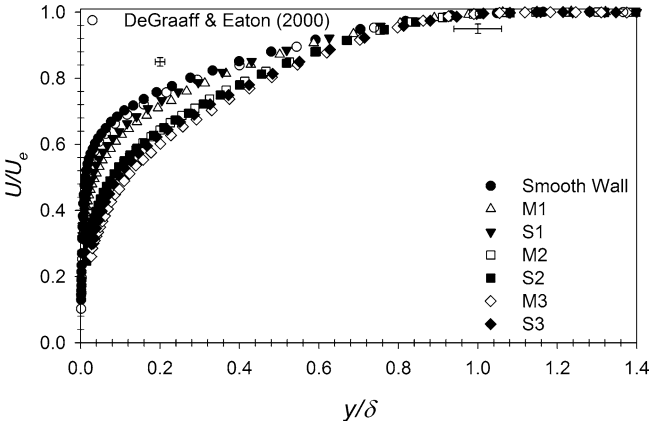

Fig. 2 Mean velocity profiles for all test surfaces (overall uncertainty: U/U_e, ±1.5%; y/δ, ±6%)

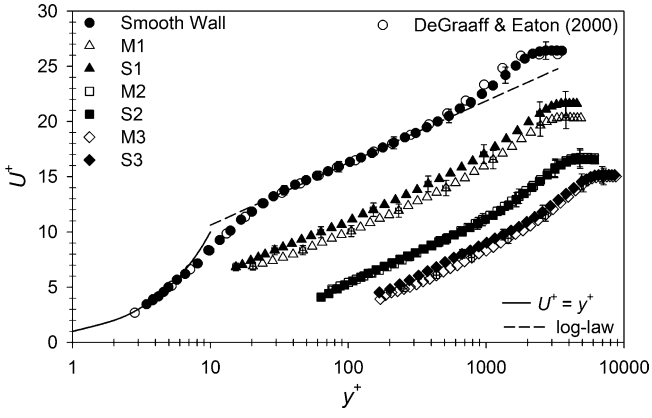

Fig. 3 Mean velocity profiles for all test surfaces in inner variables (overall uncertainty: U^+, ±3% for smooth wall and ±5% for rough walls; y^+, ±3% for smooth wall and ±5% for rough walls)

roughness height and roughness type play an important role in determining ΔU^+. For example, the M2 and S2 surfaces display almost identical roughness functions while the roughness height (k) for the S2 surface is almost 30% larger than for the M2 surface.

Velocity-defect profiles for all of the test surfaces normalized by U_τ from the Clauser chart method are shown in Fig. 4a. The present results for both the smooth and rough walls display excellent collapse to a single curve. The agreement with the smooth wall results of DeGraaff and Eaton (2000) is also good. In order to more critically assess the agreement of velocity-defect profiles in the overlap region, the profiles are presented using log-normal axes in Fig. 4b. Agreement of the present results within experimental uncertainty is again seen for $0.02 \le y/\delta \le 1$. Any differences observed appear to be due to the variability in the wake strength mentioned earlier. For example, Fig. 4c shows the expected effect of changes in wake strength on the velocity-defect profile. The figure was created by plotting Eq. 10 using the wake function of Granville (1976), given as

$$\omega(\eta) = 6\eta^2 - 4\eta^3. \tag{14}$$

The velocity defect is plotted for $\Pi = 0.38$ and 0.48 to cover the range of Π observed in the present experimental results. The variation between the profiles is similar to that observed in the experimental data. It should be stressed, however, that no definitive trend in the wake strength with increasing roughness can be discerned in the present results (Table 1) and, within their uncertainty, the results support the concept of a universal velocity defect for a wide range of relative roughness. This implies that roughness effects on the mean flow are confined to the near wall region. The existence of a universal velocity-defect profile in internal flows is supported by the recent rough wall studies of Shockling et al. (2005) and Bakken et al. (2005) in pipe and channel flows, respectively. A universal velocity-defect profile for zero pressure gradient turbulent boundary layers is supported by many studies including Hama (1954), Bandyopadhyay (1987), and Flack et al. (2005). However, the studies of Akinlade et al. (2004) and Krogstad et al. (1992) contend that roughness effects on the mean flow are observed well into the outer layer.

One of the difficulties of assessing the validity of velocity-defect scaling in turbulent boundary layers as compared to internal flows is the accurate determination of U_τ. In fully developed internal flows, the friction velocity can be reliably determined using the streamwise pressure gradient. This is independent of assumptions about the mean velocity profile, such as the existence of the log-law. For this reason, the total stress method, which makes no assumption of a linear log-law, was also used to determine U_τ in the present study. Velocity-defect profiles for all of the test surfaces normalized by U_τ obtained using the total stress method are shown in Fig. 5a. The results for both the smooth and rough walls

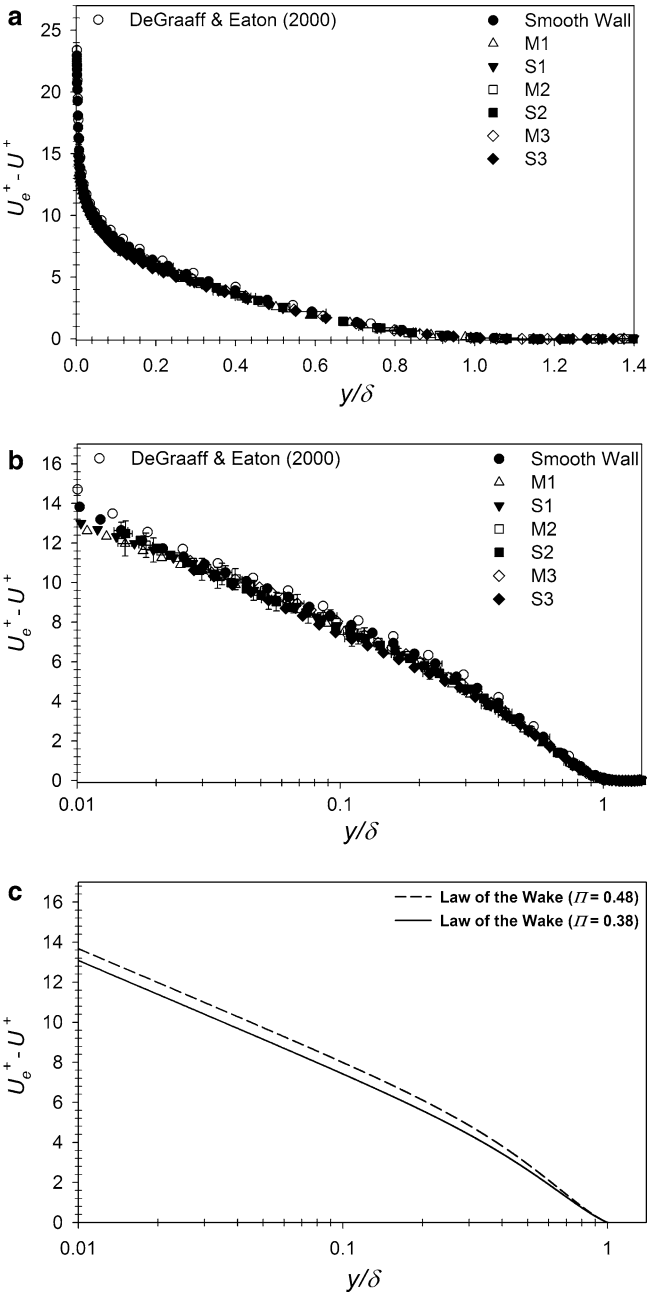

Fig. 4 Mean velocity profiles for all test surfaces in velocity-defect form using the friction velocity determined by the Clauser chart method (overall uncertainty: $(U_e–U)/U_\tau$, ±3% for smooth wall and ±5% for rough walls; y/δ, ±6% for all surfaces). **a** Normal axes, **b** log-normal axes, and **c** effect of variation in Π

show excellent collapse. These velocity-defect profiles are presented in log-normal axes in Fig. 5b. Agreement of both the smooth and rough wall results within experimental uncertainty is observed for $0.02 \le y/\delta \le 1$.

The validity of velocity-defect scaling using normalization with the velocity scale proposed by Zagarola and Smits (1998) was also evaluated. This velocity scale ($U_e\delta^*/\delta$) is independent of an accurate determination of the wall shear stress. Velocity-defect profiles for all test

surfaces normalized with Zagarola and Smits scaling are presented in Fig. 6a. The collapse of the velocity profiles using this scaling is very good. These profiles are presented in log-normal axes in Fig. 6b. Agreement of all of the profiles within experimental uncertainty is seen for $0.02 \leq y/\delta \leq 1$. In the outer layer, the collapse of the profiles seems to be improved using this scaling, and excellent collapse is observed for $y/\delta > 0.2$. However, the collapse of smooth and rough wall results in the overlap region appears to be not as good as when normalizing with U_τ. The present results agree with the findings of Akinlade et al. (2004), which showed that velocity-defect profiles for rough and smooth walls normalized with $U_e\delta^*/\delta$ follow a universal curve in the outer layer. Since both U_τ and $U_e\delta^*/\delta$ are observed to collapse the present velocity-defect profiles in the outer layer, it suggests that a friction law based on the Zagarola and Smits (1998) scaling may be possible.

6 Conclusions

Turbulent boundary layer measurements were made over a smooth wall and two types of rough walls with a wide range of relative roughness. The present results show that the mean velocity profiles for all the test surfaces agree within their uncertainty in velocity-defect form in the overlap and outer layer when normalized by U_τ. This is the case for U_τ obtained using both the Clauser chart and the total stress methods. The velocity-defect profiles also agree within experimental uncertainty when normalized with $U_e\delta^*/\delta$ as proposed by Zagarola and Smits (1998). The present results provide evidence that roughness effects on the mean flow are confined to the inner layer even for relatively large roughness. The relative roughness tested here ($16 \leq \delta/k \leq 110$ and $6 \leq \delta/k_s \leq 91$) goes beyond the criteria proposed by Jiménez (2004) and Flack et al. (2005) of $\delta/k \geq 40$ and $\delta/k_s \geq 40$, respectively, for outer layer similarity. Therefore, the concept of outer layer similarity in terms of the mean velocity profile appears to be quite robust. Further investigation is needed to determine if the turbulence structure in the outer layer is universal over the same relative roughness range. Common sense dictates that eventually a large enough roughness will act as an obstacle to the flow, resulting in a lack of mean flow similarity. This may not occur suddenly at some values of δ/k or δ/k_s , but instead gradually as δ/k is reduced and will likely be dependent

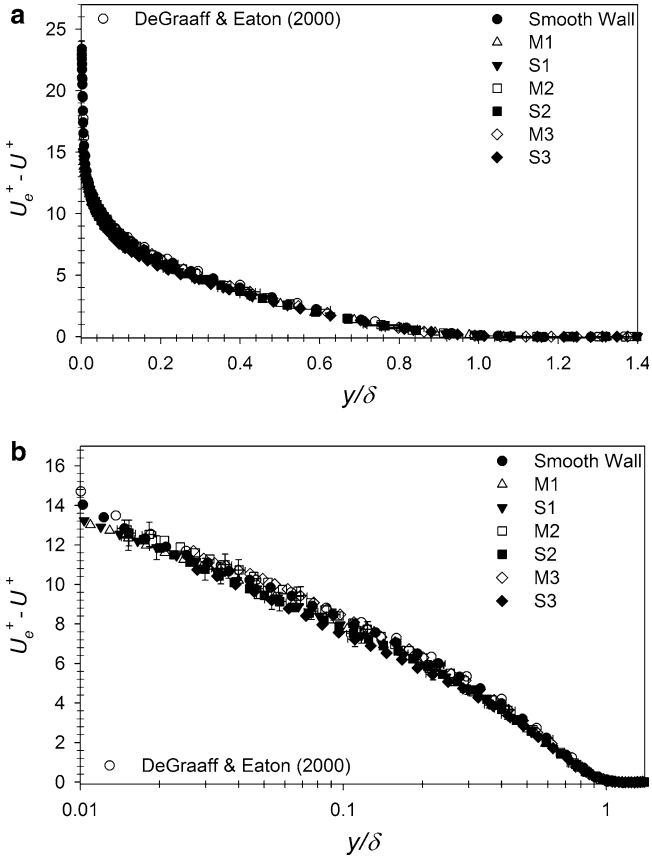

Fig. 5 Mean velocity profiles for all test surfaces in velocity-defect form using the friction velocity determined by the total stress method (overall uncertainty: $(U_e–U)/U_\tau$, ±7%; y/δ, ±6%). **a** Normal axes, **b** log-normal axes

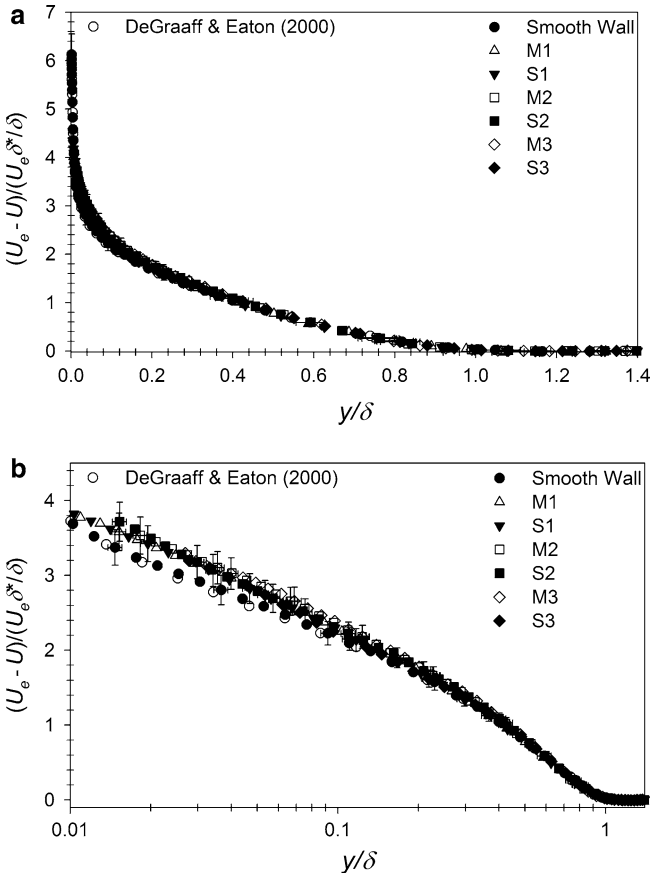

Fig. 6 Mean velocity profiles for all test surfaces in velocity-defect form using the normalization proposed by Zagarola and Smits (1998) (overall uncertainty: $(U_e–U)/(U_e\delta^*/\delta)$, ±7%; y/δ, ±6%). **a** Normal axes, **b** log-normal axes

on roughness type and density. It should be stressed that the boundary layers tested here all displayed streamwise self-similarity in the velocity-defect profile at the location of the measurements. There may be a practical limit as to how low a value of δ/k may be generated experimentally while still allowing the boundary layer to reach streamwise self-similarity. For example, increasing k also increases the boundary layer growth rate, and at some point an increase in development length may be required for the velocity defect to adjust to such a large perturbation and display streamwise self-similarity. In this way, requiring streamwise self-similarity may effectively limit how small δ/k may be. Similarity in the velocity-defect profiles between smooth and rough walls may only fail when the rough wall has not yet reached streamwise self-similarity. Further study of the evolution of boundary layers over a range of roughness heights is needed to better understand this.

Acknowledgements The authors would like to acknowledge the Office of Naval Research for the financial support of this research. Thanks go to Mr. Bill Beaver, Mr. Don Bunker, Mr. Steve Enzinger, Mr. John Zseleczky, and the rest of the USNA Hydromechanics Lab staff for their valuable help in providing technical support for the project.

References

Acharya M, Bornstein J, Escudier MP (1986) Turbulent boundary layers on rough surfaces. Exp Fluids 4:33–47

Akinlade OG, Bergstrom DJ, Tachie MF, Castillo L (2004) Outer flow scaling of smooth and rough wall turbulent boundary layers. Exp Fluids 37:604–612

Bakken OM, Krogstad P-Å, Ashrafian A, Andersson HI (2005) Reynolds number effects in the outer layer of the turbulent flow in a channel with rough walls. Phys Fluids 17, Article #065101

Bandyopadhyay PR (1987) Rough-wall turbulent boundary layers in the transition regime. J Fluid Mech 180:231–266

Clauser FH (1954) Turbulent boundary layers in adverse pressure gradients. J Aeronaut Sci 21:91–108

Coleman HW, Steele WG (1995) Engineering application of experimental uncertainty analysis. AIAA J 33:1888–1896

Coles DE (1956) The law of the wake in the turbulent boundary layer. J Fluid Mech 1:191–226

Coles DE (1962) The turbulent boundary layer in a compressible fluid. The Rand Corp. Rep. R-403-PR

DeGraaff D B; Eaton J K (2000) Reynolds-number scaling of the flat-plate turbulent boundary layer. J Fluid Mech 422:319–346

Edwards RV (1987) Report of the special panel on statistical particle bias problems in laser anemometry. J Fluids Eng 109:89–93

Flack KA, Schultz MP, Shapiro TA (2005) Experimental support for Townsend's Reynolds number similarity hypothesis on rough walls. Phys Fluids 17, Article #035102

Granville PS (1976) A modified law of the wake for turbulent shear layers. J Fluids Eng 98:578–580

Hama FR (1954) Boundary-layer characteristics for rough and smooth surfaces. Trans SNAME 62:333–351

Jiménez J (2004) Turbulent flow over rough walls. Annu Rev Fluid Mech 36:173-196

Keirsbulck L, Labraga L, Mazouz A, Tournier C (2002) Surface roughness effects on turbulent boundary layer structures. J Fluids Eng 124:127–135

Krogstad P-Å, Antonia RA (1999) Surface roughness effects in turbulent boundary layers. Exp Fluids 27:450–460

Krogstad P-Å, Antonia RA, Browne LWB (1992) Comparison between rough- and smooth-wall turbulent boundary layers. J Fluid Mech 245:599–617

Ligrani PM; Moffat RJ (1986) Structure of transitionally rough and fully rough turbulent boundary layers. J Fluid Mech 162:69–98

Millikan CM (1938) A critical discussion of turbulent flows in channels and circular tubes. Proceedings of the fifth international congress on applied mechanics, Cambridge, MA, pp 386–392

Moffat RJ (1988) Describing the uncertainties in experimental results. Exp Thermal Fluid Sci 1:3–17

Nikuradse J (1933) Laws of flow in rough pipes. NACA Technical Memorandum 1292

Patel VC (1998) Perspective: flow at high Reynolds number and over rough surfaces—Achilles heel of CFD. J Fluids Eng 120:434–444

Perry AE, Li JD (1990) Experimental support for the attached-eddy hypothesis in zero-pressure gradient turbulent boundary layers. J Fluid Mech 218:405–438

Raupach MR, Antonia RA, Rajagopalan S (1991) Rough-wall turbulent boundary layers. Appl Mech Rev 44:1–25

Schlichting H (1979) Boundary-layer theory, 7th edn. McGraw-Hill, New York

Schubauer GB, Tchen CM (1961) Turbulent flow. Princeton University Press, Princeton

Schultz MP, Flack KA (2003) Turbulent boundary layers over surfaces smoothed by sanding. J Fluids Eng 125:863–870

Schultz MP, Flack KA (2005) Outer layer similarity in fully rough turbulent boundary layers. Exp Fluids 38:328–340

Shockling MA, Allen JJ, Smits AJ (2005) Roughness effects in turbulent pipe flow. Under review for J Fluid Mech

Townsend AA (1976) The structure of turbulent shear flow. Cambridge University Press, Cambridge

von Kármán T (1930) Mechanishe aehnlichkeit and turbulenz. Nachr Ges Wiss Göttingen 58–76

Zagarola MV, Smits AJ (1998) Mean-flow scaling of turbulent pipe flow. J Fluid Mech 373:33–79